Arch Neurosci. 2022 October; 9(4):e123169. https://doi.org/10.5812/ans-123169.

Published online 2022 September 6. **Research Article**

New Histophatological Finding About Data Destroying Amyloid Black Holes in Hippocampus Following Olfactory Bulb Lesion Like as the Universe

Mehmet Dumlu Aydin [1,*], Ayca Aydin [2], Aybike Aydin [3], Elif Oral Ahiskalioglu [4], Ali Ahiskalioglu [4], Sevilay Ozmen [5] and Ayhan Kanat [6]

[1]Department of Neurosurgery, Medical Faculty, Ataturk University, Erzurum, Turkey
[2]Faculty of Electrotechnics, Information Technology and Computer Engineering, The Rhenish-Westphalian Technical University of Aachen, Aachen, Germany
[3]Department of Child Psychiatry, Cerrahpasa Medical Faculty, Istanbul University, Istanbul, Turkey
[4]Department of Anesthesiology and Reanimation, Medical Faculty, Ataturk University, Erzurum, Turkey
[5]Department of Pathology, Medical Faculty, Ataturk University, Erzurum, Turkey
[6]Department of Neurosurgery, Medical Faculty, Recep Tayyip Erdogan University, Rize, Turkey

[*]*Corresponding author*: Department of Neurosurgery, Medical Faculty, Ataturk University, Erzurum, Turkey. Email: nmda11@hotmail.com

Received 2022 February 07; **Revised** 2022 August 03; **Accepted** 2022 August 19.

Abstract

Background: Many infinite theories have been suggested to explain memory loss in neurodegenerative diseases. However, there is no data that iron-containing neurofibrillary networks can cause neuron death and erase the memory of neurons, just like black holes in space.

Objectives: Ths study aimed to investigate the electromagnetic properties of iron-loaded neurofibrillary networks formed in the hippocampus as a result of damage to the olfactory nerves, just like black holes in space, as well as whether they cause neuron death and memory loss.

Methods: All rats were tested with star maze performance before, 3 weeks, and 3 months after surgery. The data used in the study were obtained from the subjects in the experimental groups who had been followed up for 3 months with control (GI; n = 5), SHAM (GII; n = 5) with only frontal burr hole, and study (GIII; n = 15) animals with olfactory bulb lesion. All rats were tested with star maze performance before, 3 weeks, and 3 months after surgery. The olfactory bulbs and hippocampus of subjects were examined by stereological methods. Olfactory bulb volumes, degenerated neuron densities of the hippocampus, and numbers of hippocampal black holes were estimated quantitatively, and results were statistically analyzed by a 1-way analysis of variance (ANOVA). The properties of black holes in the brains and the universe were compared theoretically.

Results: The mean olfactory bulb volumes, degenerated neuron density, and black holes of the hippocampus were estimated as 4.43 $\pm$ 0.22 mm^3, 42 $\pm$ 9 mm^3, and 3 $\pm$ 1 mm^3 in GI, 4.01 $\pm$ 0.19 mm^3, 257 $\pm$ 78 mm^3, and 11 $\pm$ 3 mm^3 in GII, and 2.4 $\pm$ 0.8 mm^3, 1675 $\pm$ 119 mm^3, and 34 $\pm$ 7 mm^3 in GIII. All animals were tested with star maze performance before, 3 weeks, and 3 months after surgery. Latency, distance, speed, and path efficiency values of all animals were detected. The more diminished olfactory bulb volume ($P < 0.00001$) causes more apoptotic neurons and black holes in the hippocampus ($P < 0.0001$) and more memory loss in olfactory bulb lesion (OBL)-applied animals ($P < 0.005$).

Conclusions: Hippocampal black holes, which are similar to black holes in terms of their formation processes, may be responsible for neuronal losses and memory erasures in the brain by acting like black holes in space. These amyloid plaques, which cause neuron death and memory loss, will be called data-deleting amyloid black holes (DADA-Black Holes) in the paper.

Keywords: Hippocampus, Olfaction, Memory Loss, Black Hole, DADA-B

1. Background

Olfactory dysfunction, depression, mood-sleep disorders, and altered cortical functions have been commonly observed in patients with primordial manifestations of neurodegenerative diseases of the central nervous system (CNS), including olfactory dysfunction, depression, mood-sleep disorders, and altered cortical functions. Hyposmia and neurocognitive disorders are known as the first manifestation of neurodegenerative diseases (1). Odor perception disorders and cognitive impairment are attributed to the destruction of the hippocampus, amygdala, nigrostriatal region, and piriform cortex (2). Some disorders such

as Alzheimer's disease (AD) or Parkinson's disease (PD) occur by damage to these areas. Enormous advancements have occurred in the field of diagnostic neuroradiology (3). Rapid development in novel MR technologies led to non-invasively assessing brain structures (4). Currently, medical practice has gone through moments of great renewal (5). The rapid advances in neurosurgical knowledge and technology put increased pressure on neuroscientists to process huge amounts of data (6). For example, in degenerative CNS diseases, tissue atrophy in the gray matter, hippocampus, amygdala, and basal ganglia has been detected by magnetic resonance images (MRI) (7). Iron crystals were shown in these regions in microscopic studies. In neurodegenerative diseases, due to the acid environment formed in the brain, iron 3 salts dissolve and turn into iron 3 hydroxide. Fe(OH) liberates hydrogen ions (H^+), which in turn promotes acidosis. In this acid environment, many proteins form bound iron (III) ions, a subclass of metalloproteins. Ultimately, degenerated human hippocampal tissues lead to the formation of biogenic iron oxide magnetite, which is the predominant source of magnetization in the hippocampus (8). Olfactory bulbectomy (OBX) is a commonly used experimental model known to trigger neurodegeneration and neuronal damage in the hippocampus (9). Olfactory bulbectomy triggers neurodegeneration in some parts of the brain (9). It may lead to the degeneration of substantia nigra (10, 11).

2. Objectives

This study aimed to investigate the electromagnetic properties of iron-loaded neurofibrillary networks formed in the hippocampus due to damage to the olfactory nerves, just like black holes in space, as well as whether they cause neuron death and memory loss.

3. Methods

3.1. Rat Selection and Study Groups

This study was approved by the Animal Experiment Ethics Committee of Turkey Ataturk University Faculty of Medicine. Twenty-five animals were used and divided into 4 groups as the control (GI; n = 5), SHAM (GII; n = 5; in whose frontal burr hole was performed, dura opened, but olfactory nerves were not treated), and the study group (GIV; n = 15); in this group, in addition to the burr hole, the olfactory bulbs were mechanically crushed with a clamp and followed for 3 months. A star maze performance test was performed on all animals before the experiment and once every 2 weeks at weekly intervals after the experiment for a total of 7 times a month. The analyzes of the star maze performance tests were performed after 3 months. Delay, distance, speed, and road efficiency values of all animals were determined.

Combined balanced subcutaneous anesthetic solutions were preferred to reduce pain and mortality during surgery. Isoflurane, 0.2 mL/kg, and an anesthetic combination (ketamine HCL (150 mg/1.5 mL), xylazine HCL (30 mg/1.5 mL), and distilled water (1 mL)) were preferred as inhalation anesthetics with a face mask. The frontal midline areas of the skull were shaved, and a burr hole was opened between the olfactory bulbs in the midline of the frontal bone. In GII, only a burr hole was made, but the dura was not opened. In GIII, a burr hole was made, and dura opened, but olfactory bulb lesion (OBL) was not applied. In the study group, bilateral OBL was applied with a micro clamp (GIII; n = 15) and observed for 3 months. During the 3-month experiment, all animals were observed without any medical treatment. The olfactory functions, appetite status, and weights of the animals were noted. Before surgery, all animals were humanely decapitated under general anesthesia. The whole brains of all animals were stored in 10% formalin solutions for 7 days after the necessary cleaning procedures for histological evaluation. Olfactory bulb volumes were measured macroanatomically.

3.2. Histopathological Procedures

Olfactory nerves were cut into thin sheets by taking 5 μm slices from 30 μm cross-sectional surfaces. All 30 sections were taken of each olfactory nerves fused consecutively with others to estimate the volumes of the olfactory nerves. Samples were taken from the sections. Total glomerular numbers of olfactory bulbs were studied using the fractionation method we used previously (11). Tissue sections of each block were placed on glass slides for histopathological evaluation and stained by light microscopy (11), as well as hematoxylin eosin (H&E), glial fibrillary acidic protein (GFAP), alpha-synuclein methods for analysis and estimation of the number of black holes in the hippocampus and Levy particles (11). The distribution patterns of the number of degenerated neurons in all groups were determined by an analysis of variance (ANOVA) (95% CI). After the data were calculated, the volumes of the olfactory bulbs were estimated by calculating the volume of each olfactory bulb (OB), as in our previous studies. Like our neuron prediction methods in our various papers (11), the physical dissector method was preferred to assess the number of viable and degenerate neurons in the hippocampus. A similar method was used to estimate the number of black holes in the hippocampus. Stereological methods were used to evaluate the neuron density per cubic centimeter of the olfactory bulbs. The hip-

pocampal sections, olfactory glomerulus, and hippocampus were compared statistically. To assess the iron content, 20 consecutive sections were taken at 5 μm intervals from all hippocampus of the animals, and data destroying amyloid blackholes-B (DADA-B) numbers were estimated. Fe amounts of all 3 groups were measured in 1-mm^3 section from CA1-2-3 from the remaining parts. Ferene-s (3-(2-pyridyl)-5,6-di(2-furyl)-1,2,4-triazine-5',5"-disulfonic acid disodium salt), a chromogenic compound method, was used to estimate hippocampal iron content (1×10^{-7} g/mL) as in the study of Hedayati et al. (12).

3.3. Statistical Analyses

Differences between olfactory bulb volume, number of degenerated neurons of the hippocampus, memory test scores, and black holes were compared statistically. Data were analyzed using SPSS version 12 (SPSS Inc, Chicago, Ill, USA).

A Tukey test was used to analyze the rational analysis and statistical results of the multiple results obtained, and repeated measures (RM) were tested for significance by 1-way and 2-way ANOVA methods. A 2-sample *t*-test was used both in the analysis of cognitive scores evaluating memory status and in the analysis of unpaired data. All presented error distributions used the SEM method calculated for all binomial variables (accuracy rate, where P is the fraction of correct classifications). The significant results obtained were plotted against conventional critical P values: All margins of error presented were based on SEM sampling calculated for accuracy, where P was used for all normal variables, and all binomial variables were considered a fraction of correct classifications. Differences were considered significant at $P < 0.05$.

4. Results

Blurred consciousness, signs of meningeal irritation, epileptic convulsions, seizures, fever, and respiratory and circulatory disorders were observed in the animal who died. The heart rhythm was 280 $\pm$ 15 minutes, the respiratory rhythm was 35 $\pm$ 9 minutes, and the blood oxygen concentration was 95% $\pm$ 7% in control animals. The star maze performance test showed significant memory loss in OBL-treated subjects.

4.1. Numerical Results of Star Maze Performance Scores

4.1.1. Cognitive Scores

To assess the memory capacity of the subjects, the numerical values of the training were used as described by the authors we refer to thigmotaxis = 1, passivity = 1, random = 2, circling = 3, accidental circling = 3, chaining = 3, focused = 4, corrected = 5, and direct = 6. The memory score for each phase of the experiment is also the authors' following scale of thigmotaxis = 1, passivity = 1, random = 2, circling = 3, focused search circle = 5, and focused search = 6. Subjects' scores per day and test were summed up, which was the highest performance indicator score of 6 recorded as the best memory score.

4.1.2. Histopathological Findings

Histological appearances of iron accumulated neurons in hippocampus in dead walley, the regions where these dead neurons accumulate in the hippocampus, which we call the "Valley of the Dead", iron particles in degenerated hippocampal regions, and neurofibrils included neurons in a study of animal (Figure 1). Figure 2 shows migration of iron-loaded degenerated neurons in gravity core to form data destroying amyloid black holes in the hippocampus in a study rat. Histopathological appearances of Lewy bodies with misfolded alpha-synuclein proteins were believed to be an indicator factor in PD in a study group (Figure 3). Iron-laden neurons in normal, sham, segregated neurons in gravity core to form black holes in the hippocampus, dense iron-laden cores, and data destructing DADA-B are seen in a study rat (Figure 4).

4.1.2.1. The Numerical Results of Histopathological Data

The mean olfactory bulb volumes, degenerated neuron density, and black holes of the hippocampus were estimated as 4.43 $\pm$ 0.22 mm^3, 42 $\pm$ 9 mm^3, and 3 $\pm$ 1 mm^3 in GI, 4.01 $\pm$ 0.19 mm^3, 257 $\pm$ 78 mm^3, and (11 $\pm$ 3 mm^3 in GII, and 2.4 $\pm$ 0.8 mm^3, 1675 $\pm$ 119 mm^3, and 34 $\pm$ 7 mm^3 in GIII). The more diminished olfactory bulb volume ($P < 0.00001$) causes more apoptotic neurons and black holes in the hippocampus ($P < 0.0001$) in OBL-applied animals ($P < 0.005$).

4.1.2.2. Statistical Analysis of Star Maze Scores and Groups

Latency, distance, speed, and path efficiency values of all animals are summarised in Tables 1 and 2.

Significant results marked according to conventional critical P values were as follows:

Before surgery: There were no differences between groups.

Three weeks after surgery: Control/SHAM ($P < 0.001$), SHAM/study ($P < 0.0001$), and control/study ($P < 0.0001$)

Three months after surgery: Control/SHAM ($P < 0.005$), SHAM/study ($P < 0.0005$), control/study ($P < 0.00001$)

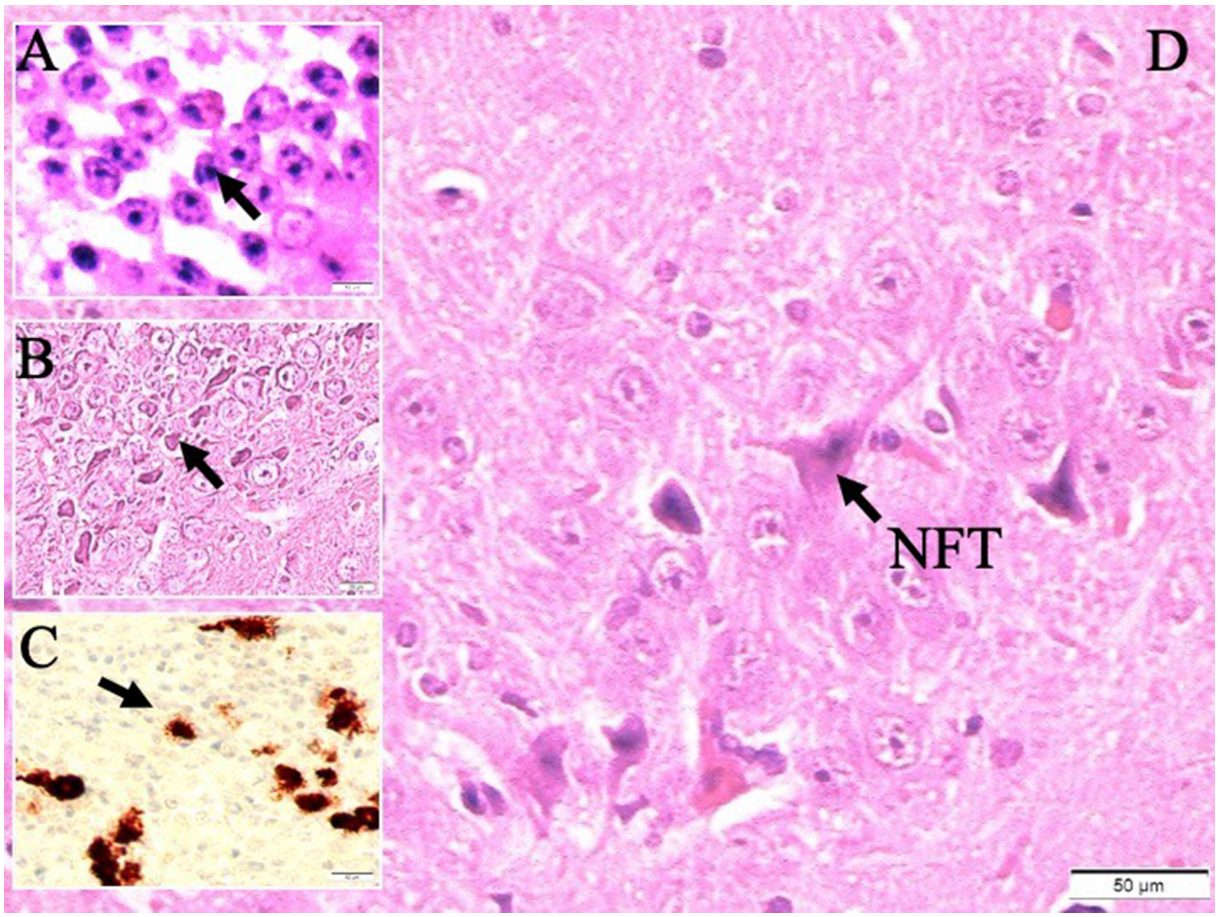

Figure 1. Histological appearances of A, iron accumulated hippocampal neurons (LM, hematoxylin eosin (H&E), × 10); B, degenerated neurons in dead walley (LM, H&E, × 10); C, iron particles in degenerated hippocampal regions (LM, H&E, × 10); D, and neurofibrils included neuron (LM, H&E, × 20) in a study rat

Table 1. Numerical Results After 2 Weeks of the Experiment [a]

Group	Latency (s)	Distance (m)	Speed (m/s)	Path Efficiency
Control (n = 5)	75 ± 17	18 ± 4	0.23 ± 0.09	0.43 ± 0.13
SHAM (n = 5)	65 ± 12	13 ± 3	0.19 ± 0.05	0.32 ± 0.11
Study (n = 15)	41 ± 9	8 ± 2	0.10 ± 0.03	0.19 ± 0.09

[a] Values are expressed as mean ± SD.

Table 2. Numerical Results After 3 Months of the Experiment [a]

Group	Latency (s)	Distance (m)	Speed (m/s)	Path Efficiency
Control (n = 5)	73 ± 16	16 ± 3	0.22 ± 0.09	0.41 ± 0.11
SHAM (n = 5)	46 ± 10	10 ± 2	0.15 ± 0.04	0.22 ± 0.09
Study (n = 15)	30 ± 6	4 ± 1	0.07 ± 0.02	0.12 ± 0.04

[a] Values are expressed as mean ± SD.

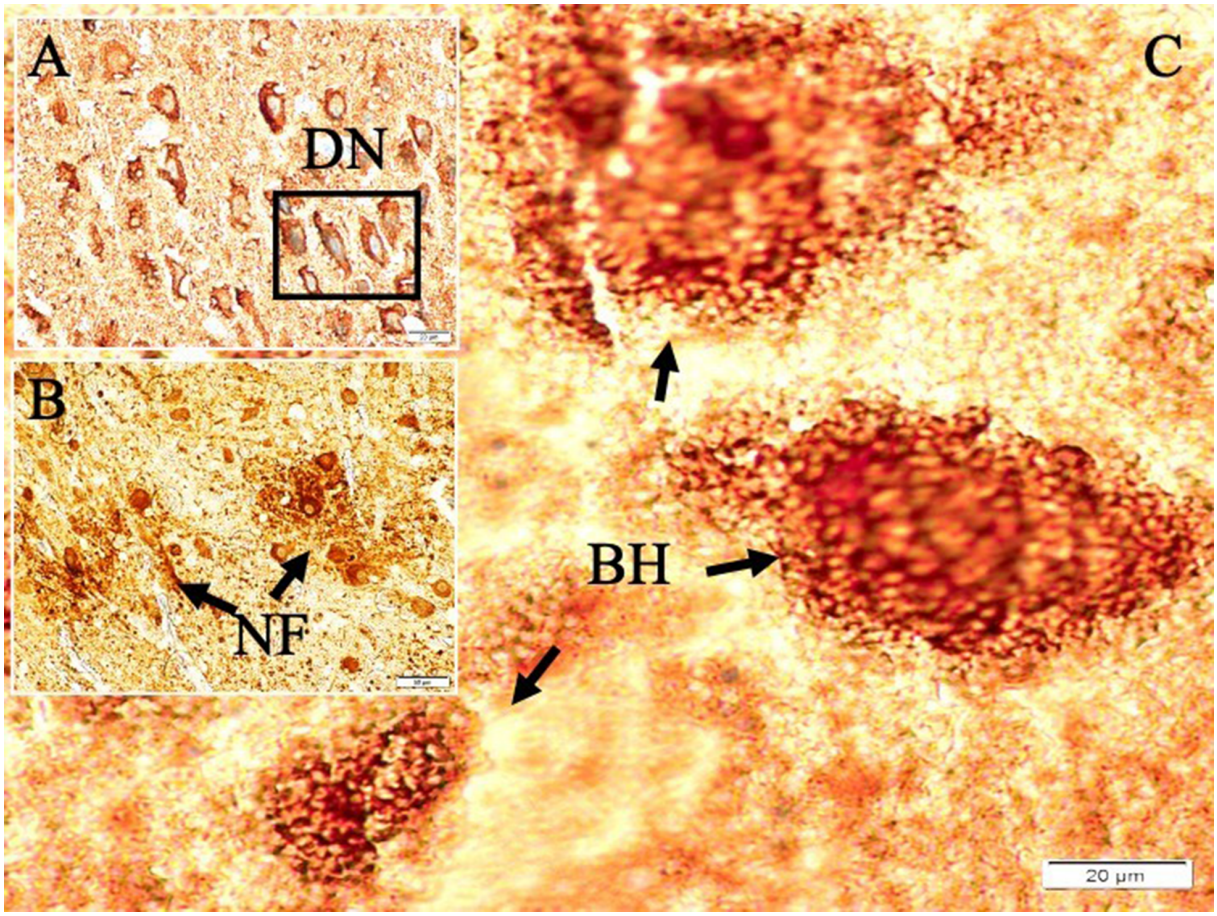

Figure 2. Iron-loaded degenerated neurons (DN) migrated to A, gravity core; B, neurofibrillary tangle forming neurons (NF) in gravity core; and C, forming black holes (BH) in the hippocampus are seen in the study rat (LM, glial fibrillary acidic protein (GFAP), × 40)

5. Discussion

5.1. Main Finding

In this study, the electromagnetic properties of iron-loaded neurofibrillary networks formed in the hippocampus due to damage to the olfactory nerves were investigated, which can cause neuron death and memory loss.

5.2. Interpretation

Safely maneuvering in the environment is central to the survival of nearly all species (13). The ability to do this depends on good learning and remembering of time and space (13). To live and reproduce in the world, all living things need a safe environment and a strong memory to build a nest, find a mate, avoid predators, return to their nests in the evening and feed their young. No animal can survive without these safety features and abilities. Therefore, every living thing needs these necessary features very effectively, which are very well developed in all mammals.

All brain parts are made up of complex circuits or networks spanning many brain regions. Brain regions that mediate this ability, such as the hippocampus and entorhinal cortex, have very good software and hardware for the management and control of this issue. The hippocampus (the main recording and storage area of memory) is essential for the continuation of such activities. Due to this feature of the hippocampus, memory studies and analytical examination of memory loss in animals are evaluated through this structure. The most widely used assessment test in this regard is the star maze test (13). We also evaluated the memory loss degrees of the subjects with this test.

The star maze performance test was used to assess the animals' memory power. The star maze test is a widely used test to evaluate hippocampal-dependent spatial learning and memory, including neurocognitive disorders such as AD. A more recent interesting water maze, the star maze, which presents some new features, was de-

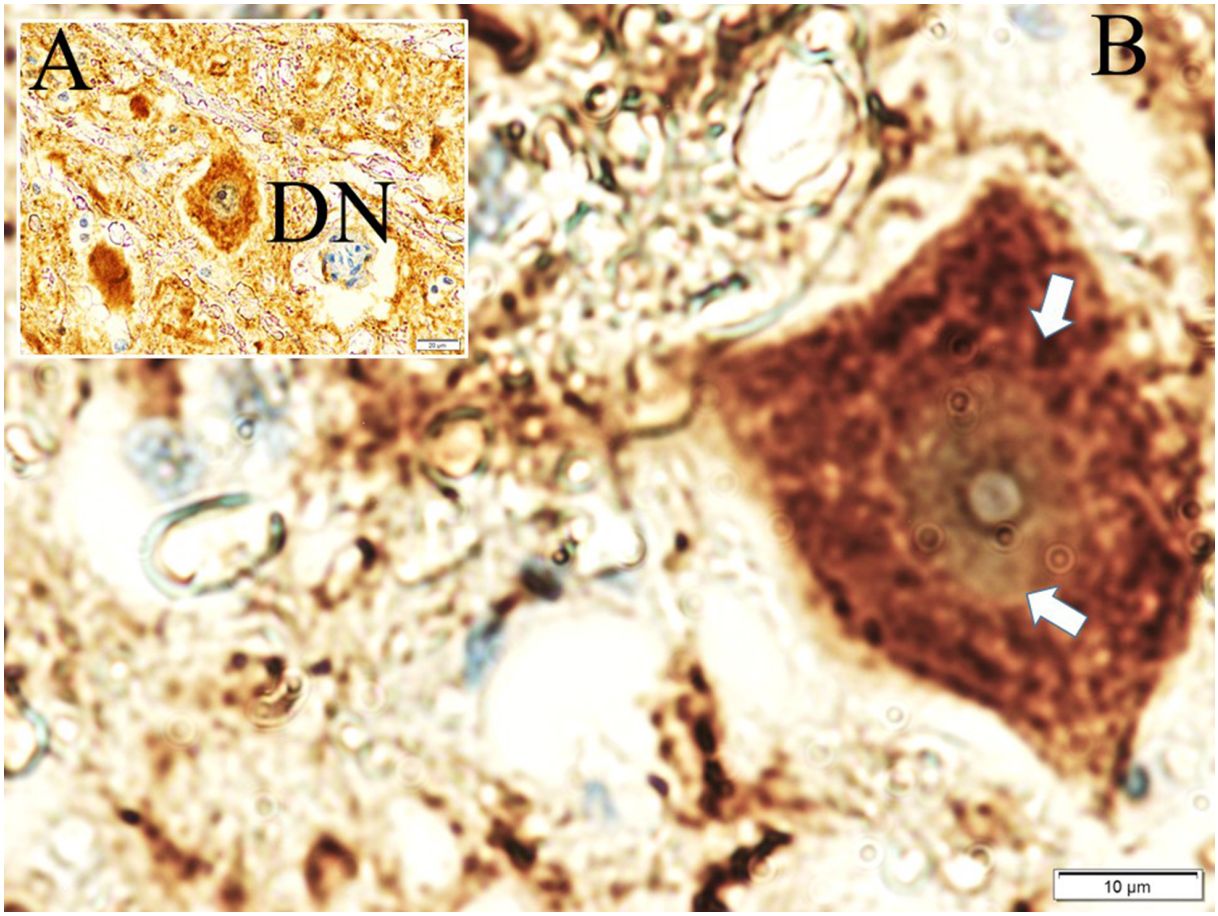

Figure 3. Histopathological appearances of A, a degenerated neuron (DN); B, Lewy bodies with misfolded alpha-synuclein proteins (white arrows) believed to be an indicator factor in Parkinson's disease (L, Alphasynuclein, × 40) in the study group

scribed by Fouquet et al. (14). Delay, distance, speed, and road efficiency values are determined by these methods, and memory scoring is done.

The brain-control circuit is closely related to dysfunction of the pyriform cortex and amygdala. Insufficient sense of smell is an important finding of AD, usually caused by a lesion in the hippocampus, amygdala, and piriform cortex. There is a definite relationship between olfactory dysfunction and nigrostriatal denervation in degenerative CNS disease. It has been suggested that the pathology of PD may begin in the olfactory bulb and anterior olfactory nucleus (10). In PD, anosmia may be detected before motor symptoms appear.

5.3. Iron Metabolism Changes in Alzheimer's Disease

Iron is the most abundant transition metal in the brain, participating in essential and diverse brain activities, such as the synthesis of neurotransmitters, myelination, and mitochondrial function (15). Excessive iron accumulation in neurons and glial cells is a serious pathogenetic mechanism in the formation of many neurodegenerative diseases such as AD, PD, and Huntington's disease (HD) (16). Iron overload has been reported by in vivo MRI in patients with AD (17). Iron deposition plays a very active role in the formation of amyloid-β aggregation (18). Alzheimer's disease patients have an abnormally high increase in iron levels in neurons in the putamen, thalamus, red nucleus, hippocampus, and temporal cortex (15). Iron accumulation in the globus pallidus and putamen, the head of the caudate nucleus, increases with age (15). The cause of brain iron accumulation with aging is uncertain (15). Iron accumulation in nerve tissues increases further during the progression of AD (15). Iron accumulation in the hippocampus and basal ganglia in rodents leads to marked impairments in spatial and aversive memory and recognition memory. Ferroptosis is an

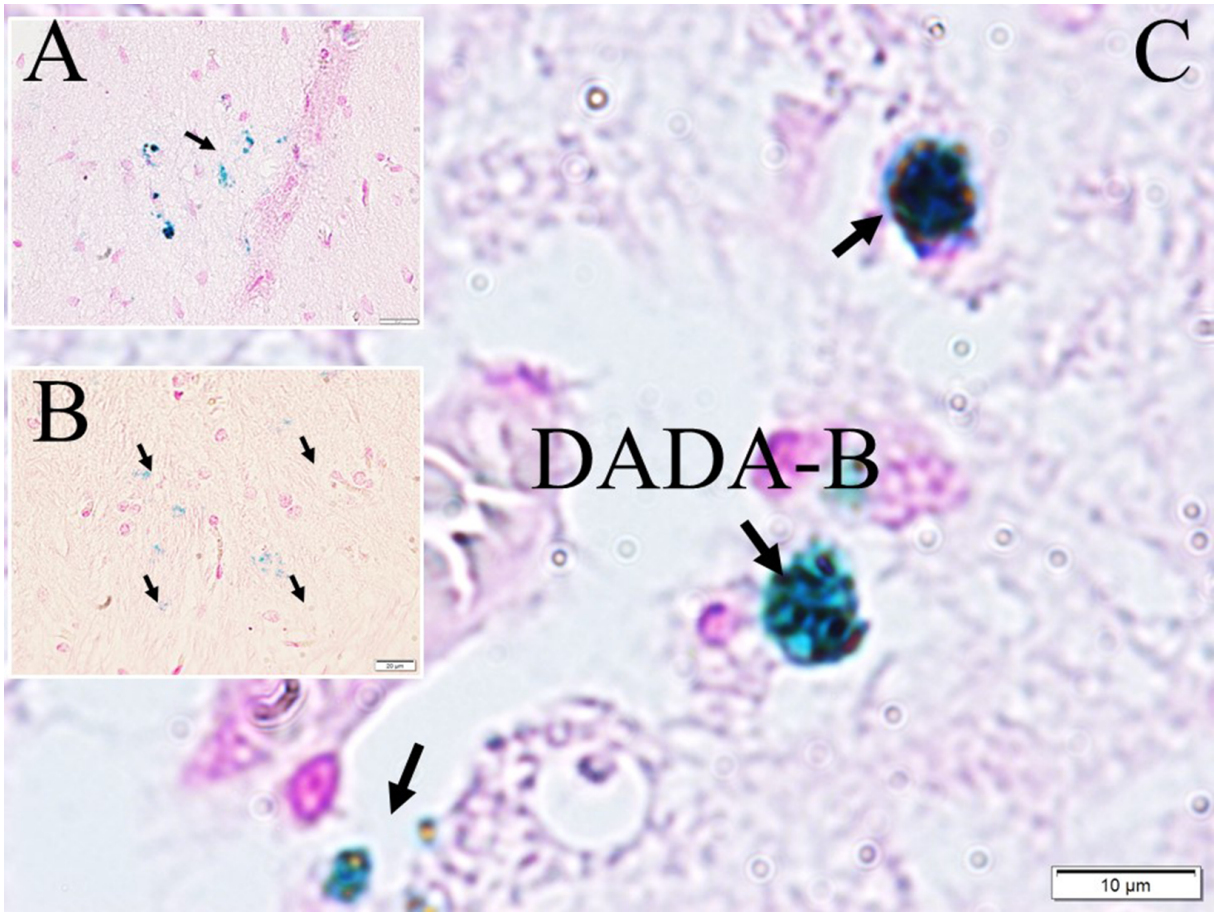

Figure 4. Iron-loaded neurons in A, a normal (black arrow; LM, Prussian Blue, × 10); B, in a sham (black arrows; LM, Prussian Blue, × 10); and C, dense and giant iron-loaded cores forming data destructing amyloid black holes (DADA-B) (black arrows, LM, Prussian Blue, × 100) are seen in a study rat.

iron-dependent cell death, which is different from apoptosis, necrosis, autophagy, and other forms of cell death (19). Ferroptosis and its cell death are observed in AD, HD, and PD, as well as degenerative diseases such as carcinogenesis, stroke, intracerebral hemorrhage, and traumatic brain injury, ischemia-reperfusion injury. Iron changes the valence state in biochemistry between the ferrous Fe^{2+} and the ferric Fe^{3+} species. While this property is vital in physiology, it can also be deleterious as a source of oxidative stress, especially in an obligate aerobic environment. Thus, iron is tightly regulated in the brain, where both deficiency and overload of iron may cause dysfunction of the brain (15).

5.4. Amyloid

The pathological features of AD and PD are neurofibrillary tangles and plaques that aggregate intraneural and consist of double-helix filaments, a microtubule-associated protein called tau, which is phosphorylated as dark structures in many regions. Amyloid plaques are extracellular and consist largely of round diffuse structures of a protein called amyloid β-protein. Beta-amyloid is a fragment of protein from amyloid precursor protein (APP) (20). Amyloid plaques are one of the hallmarks of AD. Paramagnetic iron is believed to be the main source of contrast between their plaques and surrounding tissues in T2 MRI. The amyloid plaque itself has been reported to cause no magnetic susceptibility effects. Beta-amyloid aggregations are known to increase electron density, causing local sensitivities large enough to contrast with surrounding normal tissues. Given the lack of dramatic success in clinical trials of a focus on pathological amyloid and tau, additional targets are of great interest (21).

5.5. Iron and Acidosis

Almost all living organisms store iron in the form of microscopic crystals of Fe^{3+} oxide hydroxide, 3 to 8 nm in

diameter, in ferritin, a protein from which it can be recovered if needed. All known life forms are dependent on iron and require iron in the form of oxyhemoglobin, ferredoxin, and cytochromes. Many proteins in living things contain Fe^{3+} ions bound to themselves; they are an important subclass of metalloproteins. Soluble Fe^{3+} salts tend to hydrolyze when dissolved in pure water, producing the Fe^{3+} hydroxide Fe(OH) and releasing hydrogen ions H^+ into the solution by lowering the pH until an equilibrium is reached. $Fe^{3+} + 2\ H_2O \rightleftharpoons FeO(OH) + 3\ H^+$. Consequently, concentrated solutions of Fe^{3+} salts are highly acidic. Iron is more soluble at lower pH values (22). The link between acidosis and alterations in iron metabolism needs to be explored. In an experimental subarachnoid hemorrhage study, it was reported that the cause of poor outcome might be low tissue pH levels (23) because decreasing the brain tissue pH would lead to increased iron-mediated changes.

5.6. Properties Iron Components

Biogenic iron oxide magnetite (Fe_3O_4) is the predominant source of magnetization in the hippocampus (8). Experimental studies confirmed that APPs form amyloid precipitates by binding Fe^{2+} and Fe^{3+} ions in brain areas with low temperature and low pH values. This is because Fe^{2+} and Fe^{3+} showed that APP fibrils play a key role in folding and aggregation. Fe^{3+} has a greater function than Fe^{2+} in intermolecular interactions and flocculation of APP fibers. APP clumps formed in this way exhibit high electromagnetic properties. This is because the accumulated elemental iron and Fe^{3+} are paramagnetic. Ferromagnetic materials are solid and are strongly attracted by the external magnetic field. Although ferromagnetic materials are permanent magnets, they do not lose their magnetic properties when the external magnetic field is removed. Ferromagnetic materials tend to move from the weaker part of the magnetic field to the stronger part. The magnetic susceptibility of ferromagnetic materials is positive and large. Paramagnetic materials are attracted, while diamagnetic materials are repelled by external magnetic fields. Paramagnetic materials have at least 1 unpaired electron in the system, but diamagnetic materials have paired electrons. The magnetic field direction of the magnetic field created by paramagnetic materials is outward, but the magnetic field generated by diamagnetic materials has a direction opposite to the external magnetic field. Paramagnetic materials exhibit a stronger magnetic behavior exhibited only by selective materials, while diamagnetic materials generally exhibit a weak magnetic field behavior exhibited by all materials and are easily suppressed in the presence of stronger magnetic properties.

These substances are inert and strongly attracted by the external magnetic field. Ferromagnetic materials do not lose their magnetism when the external magnetic field is removed. Ferromagnetic material tends to move from the weaker part of the field to the stronger part. A ferromagnetic material is strongly magnetized in the same direction as the field. The magnetic susceptibility of ferromagnetic material is positive and large. The ferromagnetic material can become paramagnetic when heated.

5.7. Iron Content Estimation with Electroencephalography

The function of CNS processes is highly dependent on iron-containing enzymes and proteins (24). Therefore, iron deficiency may result in changes in human behavior. Exploring electroencephalography (EEG) alpha oscillations has generated considerable interest, particularly regarding the role they play in the physiological aspects of human life (24). P300 reflects these neural activities that are related to perception, attention, decision-making processes, and updating memory related to discrete events (25). The proper functioning of brain cells relies on an abundant and continuous supply of oxygen (26). Cognitive function is impaired, and P300 latency is prolonged in acute isovolemic anemia and acute hypoxia (25). From the pyramidal cell layers of the CA1 region of the hippocampus and dentate granule cells, highly synchronized bursts of sinusoidal waves at an intensity of 4 - 7 Hz can be recorded via induction neuronal electrical activity. The information encoded in the hippocampal structure reflects an electromagnetic phenomenon of the information in the memory with these waves. Abnormal iron homeostasis in these structures can induce cellular damage through hydroxyl radical production and inhibit signaling activity by causing iron accumulation. Magnetic resonance images can often identify these changes, which are potential diagnostic biomarkers of neurodegenerative diseases. Iron chelators can cross the blood-brain barrier, penetrate cells, and reduce excessive iron accumulation, thereby providing neuroprotection.

5.8. Iron Content Estimation with Magnetic Resonance Images

Brain iron deposition has been linked to several neurodegenerative conditions. Brain MRI analyses of AD have shown higher concentrations of iron oxide and magnetite Fe^{3+} particles smaller than 20 nm in diameter and containing Fe^{2+} ions (27). As the magnetic field strength increases in the hippocampus, an increase in the amount of iron-dependent contrast agents is observed in MRI analyzes. Postmortem brain MRI of these patients showed high iron concentrations (16) and amyloid-β aggregation (18) in the hippocampus, amygdala, substantia nigra, red

nucleus, cortex, and white matter of the brain. Diamagnetic susceptibility of beta-amyloid masses can also be observed in brain samples of AD patients (20). Autopsy studies have also shown that the accumulation of $Fe^{2+/3+}$ in the hippocampus causes electromagnetic artifacts in MRI of AD (28). Fe^{2+} and Fe^{3+} iron ions show significantly different relaxation behaviors on MRI. These features can be used to distinguish Fe^{2+} and Fe^{3+} iron ion samples (29).

5.9. Definition of Black Holes Like Masses in the Hippocampus

Aggregated APPs bind heavy metals at low pH and low temperature in the presence of Fe^{2+} and Fe^{3+} ions. Fe^{2+} and Fe^{3+} play key roles in the folding and aggregation of APPs. Fe^{3+} has a greater effect on APP folding than Fe^{3+} (30). Thus, iron, which has ferromagnetic effects, accumulates in the brain. Ferromagnetic materials tend to move from the weaker to the stronger part of the magnetic field. The ferromagnetic material is stronger than the broader forms. Elemental iron and Fe^{3+} are paramagnetic. Fe^{2+} atoms can become diamagnetic when produced by certain ligands. If Fe^{2+} creates a low-spin state, it becomes paramagnetic. However, Fe^{3+} is always paramagnetic (29). Like black, if growth becomes highly valuable due to dehydration, then it dies and can be developed into a black hole by being developed in the hippocampus. It becomes unstable to form its inner plan like a project, and it will collapse within itself (31). Data destroying amyloid blackholes-B masses also swallow the parts that take place within themselves. It consists of paths accumulated over applied time and reveals a complex electrodynamic field. Degenerated neurons of the hippocampus in AD are very rich in iron and contain ionized iron in their plasma, as in black holes. Hippocampal DADA-Bs, which are similar to black holes in terms of their formation processes, may act like black holes and cause neuron and memory losses in the brain. The formation of black holes in the universe is attributed to the collapse of dying giant stars due to their high gravitational pull, and they are observed as black bodies because they even absorb their rays (32). The formation processes of DADA-Bs are similar to the formation of black holes in the universe. In other words, giant neurons in the brain vs giant stars can be given as examples of the memory spread by EEG waves that cannot leave the inside of the neuron in response to the swallowed light of the star. This information particle or waves cannot go out of the hippocampal neuron, and a situation is observed as if the memory has disappeared. That is why they named the hippocampus DADA-B.

The spiral structure of the hippocampus and the spiral structure of the universe resemble each other. The geometrical shapes of the centers of the dying stars and the histological structures of the dying neurons are also similar. The valley of death, where the stars fall, and the valley of death formed by severed dendrites and axons in the hippocampus are similar. The laws that provide an increase in the gravitational field of the dying stars explain the secret of the collapse of the neurons with increasing mass into themselves with the same laws, with an increased gravitational force. This means that the neuron self-destructs by apoptosis. Just as the release of Fe in black holes increases, the magnetic field of the increasing mass increases and swallows more stars; in the same way, dying neurons cause more neuron death due to the Fe^{+3} they release, creating stronger DADA-B2s.

Like a black hole, any neuron will have an extremely dense mass due to dehydration or denervation, and a black hole can form when large neurons that die in the brain clump together due to their gravitational pull. When such a neuron depletes its internal energy at the end of its life, the nucleus becomes unstable and collapses in on itself, and the outer layers of the cell are destroyed, just like stars. These black holes in the brain can continue to grow, engulfing the neurons in their vicinity. Black holes may exist as small black holes before they engulf other neurons, such as stars. Since a black hole has only a few internal parameters, neurons in the vicinity of the neurons that make up DADA-B are lost, or their memories are erased by the mechanisms that Hawkins describes for black holes (32). As the black hole rotates around itself, an electromagnetic field is formed around it, and complex electrodynamics emerges due to the charges it generates around it (32). In AD, the brain is very rich in iron, and its plasma is contained in black holes, as well as ionized iron. Said properties can have an electromagnetic field and erase neuronal memory. Observational studies have identified the important pathophysiologic mechanism of diseases (4). Olfactory dysfunction in PD may be the cause, not the symptom, because there have been destructions resembling those of PD in the substantia nigra (10) and Onuf's nucleus (11). This situation also jeopardizes the hardware and software of the organs that carry out nutritional and reproductive activities.

5.10. What Is Important in This Study?

This study may open new horizons in the etiology, pathogenesis, pathology, and treatment processes of memory loss observed in neurodegenerative diseases.

5.11. Limitations

This is an animal study and does not include radiological, biochemical, and neuropsychiatric examination data. Besides, this paper did not show any new technical aspects from memory loss to treatments.

5.12. Conclusions

The study has a novel hypothesis about memory loss because of iron-containing neurophylline networks. This hypothesis was tested and confirmed by histological assays. This hypothesis, as a first step, is good but needs more studies and tests for analysis in the future.

Hippocampal black holes, which are similar to black holes in terms of their formation processes, may be responsible for neuron and memory losses in the brain by acting just like black holes. Stars dying in black holes in the universe have their mass, and due to their high gravitational force, they even swallow rays and, therefore cannot be seen. In our experiment, neurons, like stars, died in hippocampal death valleys to form DADA-s, and their software probably crashed. In other words, just as the star's light cannot leave its orbit, the EEG waves of the neuron encoding the memory of the neuron in and around DADA-B cannot go out of the horizon of DADA-B2 and cannot go beyond. For this reason, these structures were named hippocampal black holes. In summary, they called it DADA-B. Like a black hole, it can be created by the death of a large neuron in the hippocampus. Neurons whose internal energy is depleted become unstable and collapse inward on themselves, and the outer layers of the cell are destroyed and turn into a black hole. The resulting black holes continue to grow and swallow all the peripherally located neurons in the brain, like stars, their hardware, and software. Since degenerate hippocampal neurons are very rich in ionized iron, their vibration creates an electromagnetic field, and complex electrodynamics occur in the periphery. These electromagnetic field generator DADA-Bs, described for the first time in the literature, can delete neuronal information that has not been mentioned in the literature.

5.13. Future Insights

Memory deletion and upload and recall processes will be able to be copied from the brain, uploaded to the brain, transferred to other brains, stored in memory banks, and used later with nanoneurochip applications in the future.

Footnotes

Authors' Contribution: Study concept and design: M. D. A., A. A., A. A., and A. A.; acquisition of data: M. D. A., A. A., E. O. A., and S. O.; analysis and interpretation of data: M. D. A. and A. A.; critical revision of the manuscript for important intellectual content: A. K.; statistical analysis: M. D. A. and A. A.; study supervision: M. D. A.; writing: A. K.

Conflict of Interests: No conflict of interests.

Ethical Approval: The Animal Experiment Ethics Committee of Turkey Atatürk University Faculty of Medicine approved this study (https://atauni.edu.tr/tr/etik-kurul-5).

Funding/Support: No funding.

References

1. Garcia-Esparcia P, Schluter A, Carmona M, Moreno J, Ansoleaga B, Torrejon-Escribano B, et al. Functional genomics reveals dysregulation of cortical olfactory receptors in Parkinson disease: novel putative chemoreceptors in the human brain. *J Neuropathol Exp Neurol*. 2013;**72**(6):524–39. [PubMed: 23656994]. https://doi.org/10.1097/NEN.0b013e318294fd76.
2. Tarakad A, Jankovic J. Anosmia and Ageusia in Parkinson's Disease. *Int Rev Neurobiol*. 2017;**133**:541–56. [PubMed: 28802932]. https://doi.org/10.1016/bs.irn.2017.05.028.
3. Kanat A, Tsianaka E, Gasenzer ER, Drosos E. Some Interesting Points of Competition of X-Ray using during the Greco-Ottoman War in 1897 and Development of Neurosurgical Radiology: A Reminiscence. *Turk Neurosurg*. 2021. [PubMed: 34859828]. https://doi.org/10.5137/1019-5149.JTN.33484-20.3.
4. Polat HB, Kanat A, Celiker FB, Tufekci A, Beyazal M, Ardic G, et al. Rationalization of Using the MR Diffusion Imaging in B12 Deficiency. *Ann Indian Acad Neurol*. 2020;**23**(1):72–7. [PubMed: 32055125]. [PubMed Central: PMC7001445]. https://doi.org/10.4103/aian.AIAN_485_18.
5. Gasenzer ER, Kanat A, Ozdemir V, Neugebauer E. Analyzing of dark past and bright present of neurosurgical history with a picture of musicians. *Br J Neurosurg*. 2018;**32**(3):303–4. [PubMed: 29848067]. https://doi.org/10.1080/02688697.2018.1467000.
6. Kanat A, Yazar U, Kazdal H, Yilmaz A, Musluman M. Neurosurgery is a profession. *Neurol Neurochir Pol*. 2009;**43**(3):286–8. [PubMed: 19618312].
7. Wattendorf E, Welge-Lussen A, Fiedler K, Bilecen D, Wolfensberger M, Fuhr P, et al. Olfactory impairment predicts brain atrophy in Parkinson's disease. *J Neurosci*. 2009;**29**(49):15410–3. [PubMed: 20007465]. [PubMed Central: PMC6666111]. https://doi.org/10.1523/JNEUROSCI.1909-09.2009.
8. Dobson J. Investigation of age-related variations in biogenic magnetite levels in the human hippocampus. *Exp Brain Res*. 2002;**144**(1):122–6. [PubMed: 11976766]. https://doi.org/10.1007/s00221-002-1066-0.
9. Aydin N, Ramazanoglu L, Onen MR, Yilmaz I, Aydin MD, Altinkaynak K, et al. Rationalization of the Irrational Neuropathologic Basis of Hypothyroidism-Olfaction Disorders Paradox: Experimental Study. *World Neurosurg*. 2017;**107**:400–8. [PubMed: 28797983]. https://doi.org/10.1016/j.wneu.2017.07.180.
10. Aydin MD, Kanat A, Hacimuftuoglu A, Ozmen S, Ahiskalioglu A, Kocak MN. A new experimental evidence that olfactory bulb lesion may be a causative factor for substantia nigra degeneration; preliminary study. *Int J Neurosci*. 2021;**131**(3):220–7. [PubMed: 32114876]. https://doi.org/10.1080/00207454.2020.1737049.
11. Kanat A, Aydin MD, Akca N, Ozmen S. First histopathological bridging of the distance between Onuf's nucleus and substantia nigra after olfactory bulbectomy-new ideas about the urinary dysfunction in cerebral neurodegenerative disease: an experimental study. *Low Urin Tract Symptoms*. 2021;**13**(3):383–9. [PubMed: 33331085]. https://doi.org/10.1111/luts.12371.
12. Hedayati M, Abubaker-Sharif B, Khattab M, Razavi A, Mohammed I, Nejad A, et al. An optimised spectrophotometric assay for convenient and accurate quantitation of intracellular iron from iron oxide nanoparticles. *Int J Hyperthermia*. 2018;**34**(4):373–81. [PubMed: 28758530]. [PubMed Central: PMC5871594]. https://doi.org/10.1080/02656736.2017.1354403.

13. Vorhees CV, Williams MT. Assessing spatial learning and memory in rodents. *ILAR J*. 2014;**55**(2):310–32. [PubMed: 25225309]. [PubMed Central: PMC4240437]. https://doi.org/10.1093/ilar/ilu013.
14. Fouquet C, Babayan BM, Watilliaux A, Bontempi B, Tobin C, Rondi-Reig L. Complementary Roles of the Hippocampus and the Dorsomedial Striatum during Spatial and Sequence-Based Navigation Behavior. *PLoS One*. 2013;**8**(6). e67232. [PubMed: 23826243]. [PubMed Central: PMC3695082]. https://doi.org/10.1371/journal.pone.0067232.
15. Lei P, Ayton S, Bush AI. The essential elements of Alzheimer's disease. *J Biol Chem*. 2021;**296**:100105. [PubMed: 33219130]. [PubMed Central: PMC7948403]. https://doi.org/10.1074/jbc.REV120.008207.
16. Schenck JF, Zimmerman EA, Li Z, Adak S, Saha A, Tandon R, et al. High-field magnetic resonance imaging of brain iron in Alzheimer disease. *Top Magn Reson Imaging*. 2006;**17**(1):41–50. [PubMed: 17179896]. https://doi.org/10.1097/01.rmr.0000245455.59912.40.
17. Zhu WZ, Zhong WD, Wang W, Zhan CJ, Wang CY, Qi JP, et al. Quantitative MR phase-corrected imaging to investigate increased brain iron deposition of patients with Alzheimer disease. *Radiology*. 2009;**253**(2):497–504. [PubMed: 19709998]. https://doi.org/10.1148/radiol.2532082324.
18. Spotorno N, Acosta-Cabronero J, Stomrud E, Lampinen B, Strandberg OT, van Westen D, et al. Relationship between cortical iron and tau aggregation in Alzheimer's disease. *Brain*. 2020;**143**(5):1341–9. [PubMed: 32330946]. [PubMed Central: PMC7241946]. https://doi.org/10.1093/brain/awaa089.
19. Yan HF, Zou T, Tuo QZ, Xu S, Li H, Belaidi AA, et al. Ferroptosis: mechanisms and links with diseases. *Signal Transduct Target Ther*. 2021;**6**(1):49. [PubMed: 33536413]. [PubMed Central: PMC7858612]. https://doi.org/10.1038/s41392-020-00428-9.
20. Gong NJ, Dibb R, Bulk M, van der Weerd L, Liu C. Imaging beta amyloid aggregation and iron accumulation in Alzheimer's disease using quantitative susceptibility mapping MRI. *Neuroimage*. 2019;**191**:176–85. [PubMed: 30739060]. https://doi.org/10.1016/j.neuroimage.2019.02.019.
21. Derry PJ, Hegde ML, Jackson GR, Kayed R, Tour JM, Tsai AL, et al. Revisiting the intersection of amyloid, pathologically modified tau and iron in Alzheimer's disease from a ferroptosis perspective. *Prog Neurobiol*. 2020;**184**:101716. [PubMed: 31604111]. [PubMed Central: PMC7850812]. https://doi.org/10.1016/j.pneurobio.2019.101716.
22. Hassan W, Ibrahim M, Nogueira CW, Braga AL, Mohammadzai IU, Taube PS, et al. Enhancement of iron-catalyzed lipid peroxidation by acidosis in brain homogenate: comparative effect of diphenyl diselenide and ebselen. *Brain Res*. 2009;**1258**:71–7. [PubMed: 19135432]. https://doi.org/10.1016/j.brainres.2008.12.046.
23. Kanat A, Aydin MD, Bayram E, Kazdal H, Aydin N, Omeroglu M, et al. A New Determinant of Poor Outcome After Spontaneous Subarachnoid Hemorrhage: Blood pH and the Disruption of Glossopharyngeal Nerve-Carotid Body Network: First Experimental Study. *World Neurosurg*. 2017;**104**:330–8. [PubMed: 28456740]. https://doi.org/10.1016/j.wneu.2017.04.105.
24. Dziembowska I, Kwapisz J, Izdebski P, Zekanowska E. Mild iron deficiency may affect female endurance and behavior. *Physiol Behav*. 2019;**205**:44–50. [PubMed: 30267737]. https://doi.org/10.1016/j.physbeh.2018.09.012.
25. Kececi H, Degirmenci Y. Quantitative EEG and cognitive evoked potentials in anemia. *Neurophysiol Clin*. 2008;**38**(2):137–43. [PubMed: 18423335]. https://doi.org/10.1016/j.neucli.2008.01.004.
26. Kanat A. Brain oxygenation and energy metabolism: Part 1–Biological function and pathophysiology. *Neurosurgery*. 2003;**52**(6):1508–9. author reply 1509. [PubMed: 12800841]. https://doi.org/10.1227/01.neu.0000068349.22859.c6.
27. Pankhurst Q, Hautot D, Khan N, Dobson J. Increased levels of magnetic iron compounds in Alzheimer's disease. *J Alzheimers Dis*. 2008;**13**(1):49–52. [PubMed: 18334756]. https://doi.org/10.3233/jad-2008-13105.
28. Antharam V, Collingwood JF, Bullivant JP, Davidson MR, Chandra S, Mikhaylova A, et al. High field magnetic resonance microscopy of the human hippocampus in Alzheimer's disease: quantitative imaging and correlation with iron. *Neuroimage*. 2012;**59**(2):1249–60. [PubMed: 21867761]. [PubMed Central: PMC3690369]. https://doi.org/10.1016/j.neuroimage.2011.08.019.
29. Dietrich O, Levin J, Ahmadi SA, Plate A, Reiser MF, Botzel K, et al. MR imaging differentiation of Fe(2+) and Fe(3+) based on relaxation and magnetic susceptibility properties. *Neuroradiology*. 2017;**59**(4):403–9. [PubMed: 28324122]. https://doi.org/10.1007/s00234-017-1813-3.
30. Vahed M, Sweeney A, Shirasawa H, Vahed M. The initial stage of structural transformation of Abeta42 peptides from the human and mole rat in the presence of Fe(2+) and Fe(3+): Related to Alzheimer's disease. *Comput Biol Chem*. 2019;**83**:107128. [PubMed: 31585353]. https://doi.org/10.1016/j.compbiolchem.2019.107128.
31. Wald RM. The Thermodynamics of Black Holes. *Living Rev Relativ*. 2001;**4**(1):6. [PubMed: 28163633]. [PubMed Central: PMC5253844]. https://doi.org/10.12942/lrr-2001-6.
32. Frolov V, Novikov I. *Black hole physics: Basic concepts and new developments*. **96**. Berlin/Heidelberg, Germany: Springer Science and Business Media; 2012.